2008 10th Intl. Conf. on Control, Automation, Robotics and Vision
Hanoi, Vietnam, 17–20 December 2008

Adaptive Filter for Speckle Reduction with Feature Preservation in Medical Ultrasound Images

Li Rui[1], Sun Zhuoxin[1], Zhang Cishen[2]
School of Electrical and Electronic Engineering[1, 2], School of Chemical and Biomedical Engineering[2],
Nanyang Technological University,
50 Nanyang Avenue, Singapore 639798
[1]liru0001@ntu.edu.sg, [1]su0001in@ntu.edu.sg, [2]ecszhang@ntu.edu.sg

***Abstract*—Current medical ultrasound imaging suffers from grainy type speckles, which highly degrade the image details and hence reduce the diagnosis information contained in the images. Various filtering techniques for speckle reduction were previously proposed, including the standard median and Wiener filters. However, their performances are still limited in the sense that either speckles are not fully suppressed or edges and point features are not well preserved. In this paper, we first discuss about the statistical Nakagami distribution and analytical multiplicative noise models of speckles in ultrasound images, and then we propose an adaptive filter, named as Nakagami multiplicative adaptive filter (NaMAF), based on these models for effective speckle reduction and feature preservation. Performances of the proposed adaptive filter are compared with that of standard speckle reduction filters, showing that the proposed NaMAF performs best in terms of best visual effect and largest signal-to-noise ratio (SNR) when tested on phantom and *in vivo* images and least mean-square error (MSE) when tested on simulated images.**

***Keywords*—speckle, ultrasound imaging, Nakagami distribution, multiplicative noise, adaptive filter**

I. INTRODUCTION

Speckle noise in the form of random black and white spots is a serious problem in ultrasound images that highly degrades image details. Studies have shown that the presence of speckles can reduce physicians' ability to detect lesions by a factor of eight [1]. Therefore, speckle reduction usually represents a critical pre-processing step for high quality ultrasound images, providing physicians with enhanced diagnostic ability. Without speckles, it is more possible to observe the small high contrast targets, low contrast objects, as well as tissue boundaries.

Speckle reduction techniques in ultrasound images are usually classified into two types: compounding and filtering [2]. In the compounding techniques, a series of images of one object is sampled at different times with different ultrasound frequencies or different scan directions, and subsequently merged to produce a composite image [3]. This process is known to reduce spatial resolution of the image. To overcome this disadvantage or to further reduce speckles, many posterior speckle filtering techniques have been developed. In the filtering techniques, usually a moving filter window is used to calculate the local statistics, based on which the filter is able to adjust its parameters for adaptive speckle reduction.

For images that contain speckles, a goal of enhancement is to remove the speckles without destroying important image features, such as edges and small high contrast objects. The most widely cited and applied filters include the median and Wiener filters. The median filter is a simple operation which is not based on any noise model and its performance may not be reliable. The Wiener filter with minimum mean-square error (MMSE) is an example of frequency domain based filtering algorithms [4], and its drawback is that speckles in bright regions cannot be suppressed. Essentially, both the Lee and Kuan filters form an output image by computing a linear combination of the centre pixel intensity in a filter window with the average intensity of the window [5]. Therefore, the filter achieves a balance between the direct averaging filter (in homogeneous regions) and the identity filter (where edges and point features exist). This balance depends on the coefficient of variation inside the filter window. In fact, Lee filter may be treated as a special case of the Kuan filter and they have very similar performances. The Frost filter also attempts to find a balance between averaging and the all-pass filter, but using an exponentially shaped filter kernel on a point-wise, adaptive basis [6].

Although the above mentioned speckle reduction filters are declared to be feature-preserving, there are certain known limitations. First, those filters do not take into account the multiplicative nature of speckles together with their distribution characteristics. As a result, speckle features can not be fully described and the filtering performances may not be so satisfactory. Second, the filtering effect depends largely on the size and shape of the filter window. Filters with large window size tend to smooth the image overly and blur the edges, whereas those with small window size can not fully suppress speckles.

In this paper, we introduce a new type of adaptive filter with adaptive window sizes based on the Nakagami distribution and multiplicative noise model of speckles, and we name it as NaMAF, which stands for Nakagami multiplicative adaptive filter. Different from other filters, the NaMAF operates directly on the envelope detected data which contains more information than the image data that are used to display on screen. The proposed NaMAF is verified to be able to effectively reduce speckles while preserving important image details, such as edges and small high contrast objects in *in vivo*, phantom as well as simulated images.

II. NAKAGAMI DISTRIBUTION AND MULTIPLICATIVE NOISE MODELS

Various statistical models for ultrasound backscattered signals have been proposed, including the Rayleigh, Rician, K, homodyned K, generalized K, and Nakagami distributions [7]. Among all these models, Nakagami distribution is the most general model that can cover almost all scattering conditions when combined with phase analysis. In addition, it is analytically simpler than the K distribution [8].

The Nakagami distribution is characterized by a shape parameter m and a scale parameter Ω, which is also the second moment of the distribution. The probability density function (PDF) of the speckles, $f(X)$, in the Nakagami model is given by [8]

$$f(X)=\frac{2m^m X^{2m-1}}{\Gamma(m)\Omega^m}\exp\left(-\frac{m}{\Omega}X^2\right), \tag{1}$$

where X is the random variable, Γ is the gamma function, m is the shape parameter and Ω is the scaling parameter. The shape parameter m is constrained such that $m\geq 0.5$ [8], and is given by

$$m=\frac{\Omega^2}{Var(X^2)}=\frac{\left[E\left(X^2\right)\right]^2}{E\left[X^2-E\left(X^2\right)\right]^2}, \tag{2}$$

where $Var(.)$ is the variance operator, $E(.)$ is the expectation operator, and the scaling parameter Ω is written as

$$\Omega=E\left(X^2\right). \tag{3}$$

The expected value of X^n or Nakagami n^{th} moment denoted by $E_N(X^n)$, is given by [8]

$$\mu_n=E_N\left(X^n\right)=\frac{\Gamma\left(m+n/2\right)}{\Gamma\left(m\right)}\left(\frac{\Omega}{m}\right)^{n/2}. \tag{4}$$

The Nakagami distribution mean $E_N(X)$ is calculated by setting n=1 in (4), i.e.

$$E_N(X)=\frac{\Gamma(m+0.5)}{\Gamma(m)}\sqrt{\frac{\Omega}{m}}. \tag{5}$$

Due to the fact that m is insensitive to the effects of scaling, it conveys information about the ultrasonic echo statistics and can be treated as an indicator of the scatterer concentration in the range cell [8].

Equation (1) transforms to different distributions at different m values. The special case of m = 1 indicates the presence of a large number of randomly distributed scatterers, none of which produces a significant reflection by itself [12]. Speckles are said to be fully developed. In this case, Nakagami PDF becomes Rayleigh distribution specified by [9]

$$f(X)=\frac{X}{a^2}\exp(-\frac{X^2}{2a^2}), \tag{6}$$

where a is the Rayleigh parameter estimated as

$$a=\sqrt{\frac{1}{2N}\sum_{i=1}^{N}X_i^{\,2}}=\sqrt{\frac{1}{2}E(X^2)}. \tag{7}$$

With reference to (3), (7) can be rewritten as

$$a=\sqrt{\frac{\Omega}{2}}. \tag{8}$$

Rayleigh distribution has a mean denoted as $E_R(X)$ and calculated by [14]

$$E_R\left(X\right)=a\sqrt{\frac{\pi}{2}}=\sqrt{\frac{\pi\Omega}{4}}. \tag{9}$$

By relating (5) and (9), we have

$$E_N(X)=\frac{\Gamma(m+0.5)}{\Gamma(m)}\sqrt{\frac{4}{\pi m}}E_R(X). \tag{10}$$

If we denote

$$k(m)'=\frac{\Gamma(m+0.5)}{\Gamma(m)}\sqrt{\frac{4}{\pi m}}, \tag{11}$$

then (10) becomes

$$E_N(X)=k(m)'E_R(X). \tag{12}$$

So $k(m)'$ here is the ratio of the mean of Nakagami distributed data and the Rayleigh mean at a particular scatter density reflected by m. Since Rayleigh distribution characterizes fully developed speckle condition, k' (for simplification, subscript m is omitted) can be viewed as an indicator of the speckle formation process. Looked in another way, k' can parameterize the extent to which the mean of the echo envelope is increased when the extent of speckle formation increases. To suppress speckles, one would filter more the envelope image where fully formed speckles are present (when k' is large) and less in regions where k' is small or where resolved point scatters exist (scatter densities less than 1 per resolution cell results in resolved scatters).

In addition to the above Nakagami statistical model, multiplicative noise model is also adopted by many researchers to fully describe the speckle nature [9, 16]. Speckles that appear in coherent imaging process employed by medical ultrasound imaging are caused by the destructive and constructive interferences of the backscattered signals, which provide information related to the number, mean spacing and scattering cross sections of the scatters constituting the tissue

[10]. They behave as random multiplicative noise of intensity ultrasound image X and may be expressed by [9]

$$X = Yn, \tag{13}$$

where X is the speckled image data after envelope detection, Y is the corresponding speckle-free image data, and n is the multiplicative speckle noise independent of Y with unity mean and variance σ_n^2 [9].

The mean of X is given by

$$E(X) = E(Yn) = E(Y)E(n) = E(Y), \tag{14}$$

and the variance of X is obtained as

$$\begin{aligned} \sigma_X^2 &= Var(X) = E\left[(Yn - E(Yn))^2\right] \\ &= E\left(Y^2\right)E\left(n^2\right) - \left(E(Y)\right)^2\left(E(n)\right)^2 \end{aligned}. \tag{15}$$

If the tissue reflectivity has constant average intensity, i.e. $E(Y^2) = (E(Y))^2$, together with (14), we have

$$\sigma_X^2 = \left(E(Y)\right)^2\left[E\left(n^2\right) - \left(E(n)\right)^2\right] = \mu_X^2\sigma_n^2 \tag{16}$$

Therefore, the noise standard deviation σ_n is given by

$$\sigma_n = \frac{\sigma_X}{\mu_X}. \tag{17}$$

In (17), σ_n basically indicates the amount or strength of the multiplicative noise that exists in the corrupted envelope image. The larger the σ_n is, the stronger the noise is. Therefore, one would filter more the image regions where σ_n is large. Equation (17) also provides a formula for estimation of σ_n using σ_X and μ_X.

III. Model Based Adaptive Filter with Adaptive Windowing

A. Model Based Adaptive Filter

Parameter k' in (12) derived from the Nakagami distribution model and σ_n in (17) derived from the multiplicative noise model are both indicators of the speckle noise strength in ultrasound images after envelope detection of the post-beamformed radio-frequency (RF) data. The larger the k' and σ_n are, the more the noise exists and the more desirable to filter the noise out. Therefore, it is possible to design an adaptive filter based on these parameters. An unsharp masking filter could well serve this purpose. The output y of the filter for input x is given by:

$$y(i,j) = x(i,j) - k(i,j) \times \left(x(i,j) - \bar{x}\right), \tag{18}$$

where $x(i,j)$ is the observed pixel value at position (i,j) in the centre of the sliding window, $\bar{x}$ is the mean pixel value for all pixels inside the window, $y(i,j)$ is the pixel output at position (i,j), and $k(i,j)$ within (0, 1) is the key adaptive parameter used to determine the amount of adjustment or filtering for the noisy pixel $x(i,j)$. It should be noted that when k (for simplification the subscripts i, j are omitted) is approaching 1, y is approaching $\bar{x}$, and, therefore, maximum filtering or smoothing is realized. On the contrary, when k is close to 0, y is approaching x and minimum filtering or smoothing is applied.

Based on the filtering principle described above, we could relate the k' and σ_n parameters with the adaptive filter parameter k through the following equation

$$k = \frac{k' + \sigma_n}{\max\left(k' + \sigma_n\right)}. \tag{19}$$

Equation (19) not only takes into account both speckle noise indicators k' and σ_n, but also restricts the adaptive filter parameter k within (0, 1) for proper filtering operations. The filter designed is expected to adaptively suppress speckle noise based on some local statistics or parameters. Since k is limited to the range (0, 1), the filter output will vary from no filtering to maximum filtering.

B. Adaptive Windowing

For optimal filter performances, speckle noise should be suppressed to a maximum extent without impairing the resolution and important details. Adaptive windowing technique needs to be applied for both noise reduction and detail preservation. Then it is desirable to suppress noise in homogeneous regions confined by large windows by filtering more and to preserve important features in heterogeneous regions confined by small windows by filtering less. Therefore, more regions shall be classified as homogeneous for better noise reduction. It becomes necessary to use different window sizes for different regions to make most of them, if not all, relatively homogeneous. From the definition of m in (2), m could be an indicator to distinguish between homogeneous regions and heterogeneous regions where edges or point features exist, since homogeneous regions imply small variance and hence large m, and vice versa. This was also experimentally verified in MATLAB (Fig. 1). The more homogeneous the region is, the larger m tends to be.

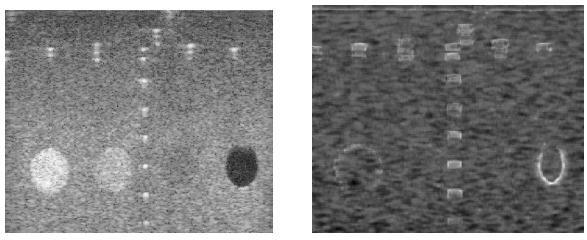

(a) (b)

Figure 1. (a) Original image. (b) Plot of log(1/m) with window size {28, 7}

Estimation of the Nakagami shape parameter m using (2) is basically affected by the applied window size. Instead of the commonly adopted square windows by other researchers, windows with shapes similar to the imaging data dimensions are used in our experiment for better filtering performances. For example, for imaging data with dimension {1032, 256},

rectangular windows of similar shapes and discrete sizes {28, 7}, {20, 5}, {12, 3}, {4, 1} are used. These four discrete windows would be good enough for region identification and filtering, since larger windows would blur the images and hence reduce resolutions while smaller windows are no longer meaningful. To choose a proper window size, threshold value m_0 of the m map for region classification obtained with the largest window size {28, 7} is first found out using the iterative algorithm described below [15]:

1. *An initial threshold m_0 is chosen randomly.*
2. *The m map is segmented into object and background pixels, creating two sets G_1 and G_2. Denote f(i, j) as the value of the pixel located in the ith column, jth row, then G_1 = {f(i, j): f(i, j) > m_0}, and G_2 = {f(i, j): f(i, j) ≤ m_0};*
3. *The average of each set G_1 and G_2 is computed and denoted as m_1 and m_2 respectively.*
4. *A new threshold m_0' is created that is the average of m_1 and m_2. i.e.*

$$m_0' = \frac{m_1 + m_2}{2}. \tag{20}$$

5. *Go back to step 2, now using the new threshold computed in step 4. Keep repeating until the new threshold matches the one before, i.e. convergence has arrived.*

Theoretically, for m smaller than the computed threshold m_0, edges or point features exist for window size {28, 7}. Then we should find a smaller window that makes the region homogeneous. If at the same position for a smaller window size {20, 5}, the new m value is greater than m_0, it implies that the current region is relatively homogeneous now, and this small window size {20, 5} shall then be adopted. Consequently, the new m is then updated and used to calculate k', one of the inputs to the adaptive filter. Otherwise, a smaller window size should be attempted until the region becomes homogeneous or the smallest window possible has been used. The above process repeats until all regions are possibly classified to be homogeneous, and all the m values are updated using pre-defined four window sizes {28, 7}, {20, 5}, {12, 3} and {4, 1}. At the same time, local statistics such as mean and variance and hence estimated noise standard deviation σ_n are also calculated correspondingly when the window sizes have changed. As a result, the filter adjusting parameter k is always kept updated for optimal adaptive filtering effects. Therefore, speckle reduction could well be done and features are expected to be well preserved.

IV. Filtering Results

A. Phantom and In Vivo Images

The experimental raw RF data were collected from an advanced ultrasound scanner SONIX RP by scanning a standard experimental phantom, and then filtered using the Butterworth filter to remove the low and high frequency system noise. The data were then envelope detected using Hilbert Transform, followed by non-linear compression for final image display on the screen. When the median, Wiener and the proposed adaptive filters are tested on the envelope detected with the aid of MATLAB simulation tool, Fig. 2 is obtained showing the comparison results. Since performances of median and Wiener filters are highly dependent on the window sizes adopted, results of using different window sizes are shown for comparison.

From Fig. 2 it can be seen that the median filter and Wiener filter with window size {3, 3} can not fully suppress speckles, while for a larger window size {7, 7}, the median filter tends to overly smooth and blur the image details, and the Wiener filter can not suppress speckles in the bright regions. In comparison, the proposed NaMAF filter can effectively reduce speckles in homogeneous regions where a large number of random scatters exist while preserving the image details such as edges and small point features in the middle of the image.

For quantitative comparison, the signal-to-noise ratio (SNR) represented by the ratio between the mean and standard deviation values of the image pixel values within the region of interest was calculated, i.e.

$$SNR = \frac{E(X)}{\sqrt{Var(X)}} = \frac{E(X)}{\sqrt{E\left((X - E(X))^2\right)}}. \tag{21}$$

The SNR in the homogeneous regions is a good measure of speckle strength. The higher the SNR is, the less the speckle noise and the better the speckle reduction effect is. When SNR was measured in three homogeneous regions of size {50, 20}, i.e. a dark region (Region 1), a gray region (Region 2) and a bright region (Region 3), Table I shows the comparison results for images processed by different speckle reduction filters. It can be seen that the proposed NaMAF can achieve highest SNR in homogeneous regions compared to the median and Wiener filters with different window sizes; that is, NaMAF has the best speckle reduction effectiveness among all the filters implemented.

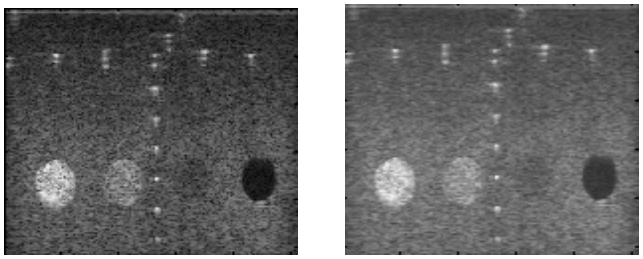

(a) Speckled (b) Median {3, 3}

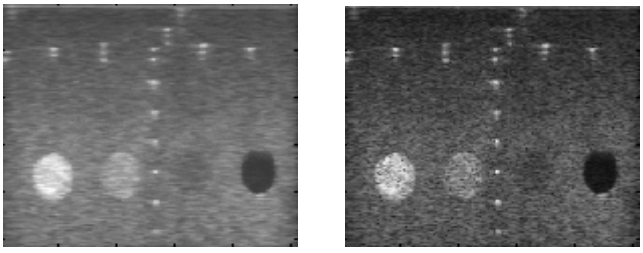

(c) Median {7, 7} (d) Wiener {3, 3}

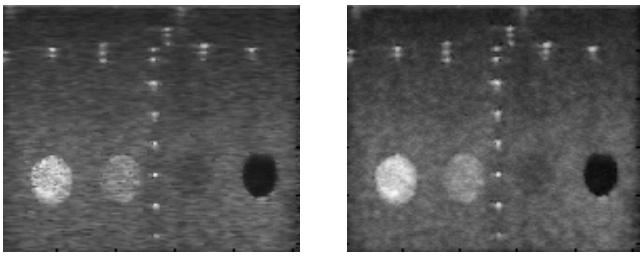

(e) Wiener {7, 7} (f) Proposed NaMAF

Figure 2. Filter performance comparison for phantom images. (a) Speckled phantom image, (b) Median filtered image with window size {3, 3}, (c) Median filtered image with window size {7, 7}, (d) Wiener filtered image with window size {3, 3}, (e) Wiener filtered image with window size {7, 7}, and (f) Proposed NaMAF filtered image.

TABLE I. SNR COMPARISON FOR PHANTOM IMAGES

SNR	Region 1	Region 2	Region 3
Speckled	6.4738	6.5391	6.7730
Median {3,3}	8.8456	8.9995	9.3808
Median {7,7}	13.4392	13.5373	15.7032
Wiener {3,3}	8.5180	7.6406	7.6972
Wiener {7,7}	13.8067	10.0227	9.2184
Proposed NaMAF	**16.6575**	**17.2393**	**16.8082**

In order to examine the edge and point preserving capability of the proposed NaMAF, Fig. 3 plots the original and NaMAF filtered data along the two columns across the edges, and point features respectively.

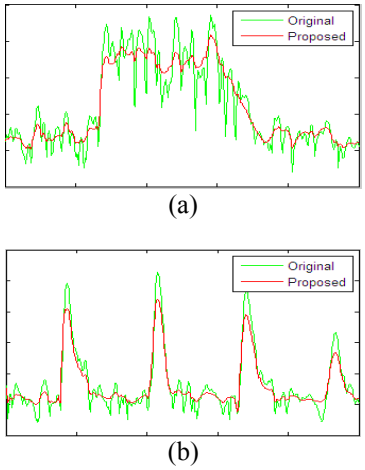

(a)

(b)

Figure 3. Data plot across (a) edges, and (b) small high contrast objects

It can be seen that the data processed by the proposed adaptive filter remains sharp at edges in Fig. 3(a) and keeps the high contrast in Fig. 3(b). Compared to the original speckled image, the proposed adaptive filter could reduce speckles effectively in homogeneous regions and at the same time preserve the edges and point features well.

For further performance comparison, some *in vivo* images were also tested. Fig. 4 shows the speckled image as well as images with different filters applied, and Table II shows the SNR values calculated over three regions identical to those in Table I. It can be seen from both Fig. 4 and Table II that, compared to standard median and Wiener filters, the proposed NaMAF is most effective in speckle reduction and detail preservation reflected by most improved visual effect as well as highest SNR values over three representative regions.

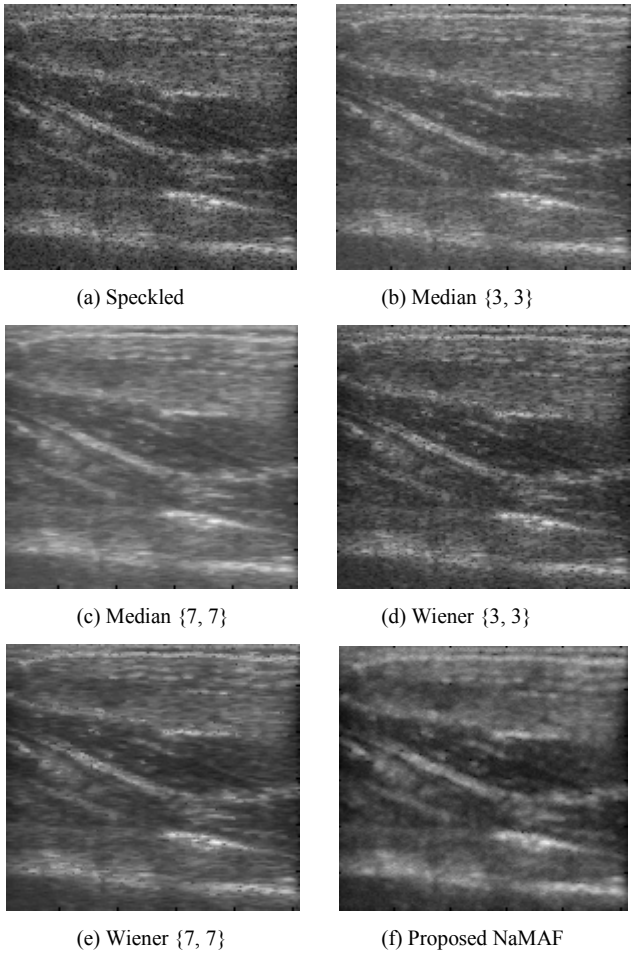

(a) Speckled (b) Median {3, 3}

(c) Median {7, 7} (d) Wiener {3, 3}

(e) Wiener {7, 7} (f) Proposed NaMAF

Figure 4. Filter performance comparison for *in vivo* images. (a) Speckled *in vivo* image, (b) Median filtered image with window size {3, 3}, (c) Median filtered image with window size {7, 7}, (d) Wiener filtered image with window size {3, 3}, (e) Wiener filtered image with window size {7, 7}, and (f) Proposed NaMAF filtered image.

TABLE II. SNR COMPARISON FOR IN VIVO IMAGES

SNR	Region 1	Region 2	Region 3
Speckled	4.3901	5.2875	5.9910
Median {3,3}	5.0006	6.3160	7.5612
Median {7,7}	6.0840	7.5410	10.7817
Wiener {3,3}	4.9806	6.1992	7.6432
Wiener {7,7}	5.8351	7.6668	11.1930
Proposed NaMAF	**6.0966**	**8.1172**	**12.4012**

B. *Simulated Images*

To better assess performances of the proposed NaMAF filter, speckles with variance 0.1 were simulated and added to some standard images using the speckle addition function *imnoise(.)* in MATLAB. Then the speckle suppression ability

and image quality after filtering are measured using the mean-square error (MSE) performance index as given below [13]

$$MSE = \frac{1}{K}\sum_{i=1}^{K}\left(\hat{S}_i - S_i\right)^2, \qquad (22)$$

where S and $\hat{S}$ are pixel values of the original and de-noised images, respectively, and K is the image size calculated by number of pixels.

MSE actually measures the closeness of the image after speckle reduction to the original real speckle free image. Since for ultrasound images there is actually no "original" speckle-free image for comparison, this measure can not be applied for assessing quality of ultrasound images. Instead, it can only be used to quantify the quality of simulated images, where the original image is available. The smaller the MSE value is, the better the speckle reduction filter performs. Fig. 5 below shows the MSE comparison result for the simulated images, where *Image1* and *Image2* are the standard MATLAB images "*cameraman.jpg*" and "*lena.gif*" respectively.

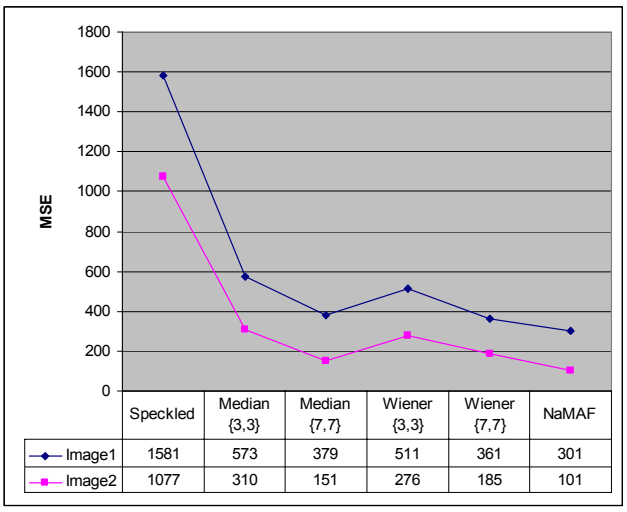

	Speckled	Median {3,3}	Median {7,7}	Wiener {3,3}	Wiener {7,7}	NaMAF
Image1	1581	573	379	511	361	301
Image2	1077	310	151	276	185	101

Figure 5. MSE comparison for different filters.

From Fig.5 it can be seen that the MSE for the speckled images are the largest for both images while MSE for images filtered by the proposed NaMAF have the smallest values among all the filters tested. This, to a great extent, means that NaMAF has strong image restoration capability for images corrupted by speckle noise, which is multiplicative and follows Nakagami distribution in nature. As a result, NaMAF outperforms other known filters, such as the median and Wiener filters, in terms of both speckle reduction and feature preservation.

V. CONCLUSIONS

An adaptive filter NaMAF based on Nakagami speckle distribution model and multiplicative noise model was developed to reduce speckles in ultrasound images. When tested on the phantom, *in vivo* as well as simulated images, the proposed NaMAF filter was demonstrated to outperform other commonly used standard speckle reduction filters, such as the median and Wiener filters, in terms of both speckle suppression in homogeneous regions and feature preservation in non-homogeneous regions that contain edges and point features.

ACKNOWLEDGMENT

We wish to acknowledge the funding support for this project from Nanyang Technological University under the Undergraduate Research Experience on Campus (URECA) programme. We would also like to thank Mr. Liang Dayang in Nanyang Technological University for his help in implementing some MATLAB functions used in the work of this paper.

REFERENCES

[1] M. E. Anderson and G. E. Trahey. "A seminar on k-space applied to medical ultrasound." [Online]. Available: http://dukemil.egr.duke.edu/Ultrasound/k-space/ [Accessed: Apr 10, 2008]

[2] T. Eltoft. "Modeling the amplitude statistics of ultrasonic images." IEEE Transactions on Medical Imaging, Vol. 25, No.2. 2006.

[3] P. C. Li. "Compounding method for reducing speckle noise." U.S. Patent 6 517 486, Aug. 16, 2001.

[4] J. F. Xiao, J. Li, and A. Moody. "A detail-preserving and flexible adaptive filter for speckle suppression in SAR imagery." *International Journal of Remote Sensing*, vol. 24, no. 12, 2451-2465, 2003.

[5] J. Lee, "Digital Image Enhancement and Noise Filtering by Use of Local Statistics." IEEE Transactions on Pattern Analysis and Machine Intelligence, vol. 2, no. 2, pp. 165-168, 1980.

[6] V. Frost, J. Stiles, K. Shanmugan, and J. Holtzman, "A model for radar images and its application to adaptive digital filtering and multiplicative noise," IEEE Transactions on Pattern Analysis and Machine Intelligence, vol.4, pp. 157-166, Mar. 1982.

[7] L. Clifford, P. Fitzgerald, and D. James. "Non-Rayleigh First-Order Statistics of Ultrasonic Backscatter from Normal Myocardum." *Ultrasound in Med. And Biol.* 19: 487-495. 1993.

[8] P. M. Shankar. "A general statistical model for ultrasonic backscattering from tissues." IEEE Transactions on Ultrasonics, Ferroelectrics and Frequency Control 47, 727-736. 2000.

[9] J.M.Park, W.J.Song & W. A. Pearlman, "Speckle filtering of SAR images based on adaptive windowing*", IEEE Image Singal Process*, Vol 146, No 4. , 1999

[10] L. L. Fellingham, and F. G. Sommer. "Ultrasonic characterization of tissue structure in the in vivo human liver and spleen." IEEE Transactions. Sonicx Ultrason. Vol. SU-31, No. 4. 1984

[11] M. Nakagami, "The m-distribution – a general formula of intensity distribution in rapid fading", *Statistical Methods on Radio Wave Propagation*, W.C. Hoffman, Ed. New York: Pergamon Press, pp.3-36, 1960.

[12] V. Dutt, "Statisical analysis of ultrasound echo envelope", Ph.D dissertation, The Mayo Graduate School, 1995.

[13] A. Achim and A. Bezerianos. "Novel Bayesian Multiscale Method for Speckle Removal in Medical Ultrasound Images." IEEE Transactions on Medical Imaging. Vol. 20. (8). 772-783. 2001.

[14] "Rayleigh distribution." [Online]. Available: http://en.wikipedia.org/wiki/Rayleigh_distribution. [Accessed: Aug. 12, 2008]

[15] Thresholding (image processing). [Online]. Available: http://en.wikipedia.org/wiki/Thresholding_%28image_processing%29. [Accessed: Aug 28, 2008]

[16] K. D. Donohue, M. Rahmati, L. G. Hassebrook, and P. Gopalakrishnan. "Parametric and nonparametric edge detection for speckle degraded images." Optical Engineering, 32(8):1935-1946, 1993.